

# Reservoir Identification of Bac-Man Geothermal Field Based on Gravity Anomaly Analysis and Modeling

Muh Sarkowi<sup>1\*</sup> and Rahmat Catur Wibowo<sup>1</sup>

<sup>1</sup>Geophysical Engineering, Universitas Lampung, Sumantri Brojonegoro Street No.1, 35145, Lampung, Indonesia

\*Corresponding author. E-mail: [muh.sarkowi@eng.unila.ac.id](mailto:muh.sarkowi@eng.unila.ac.id)

Received: April. 05, 2021; Accepted: July. 29, 2021

The Bac-Man gravity modeling was carried out to describe the geological structures that control the geothermal system and estimate the area of the geothermal reservoir. A total of 125 data points were used to produce a complete Bouguer anomaly map of the area. The gravity data are separated into regional and residual components to enhance the structural features of the sedimentary and basement rocks in the study area. Gravity data were analyzed using gradient interpretation techniques for edge detection, such as vertical descent. To perform three-dimensional (3-D) modeling, a  $5 \times 5$  km volume and a depth of 2.5 km were selected. This study presents the interpretation of various gravity anomaly maps and 3-D inversion models. The interpretation of the vertical derivative of the gravity data indicates the presence of a low gradient anomaly. The anomaly map is used to identify several faults or intrusions compared to the faults or intrusions that are mapped. The 3-D model reveals that there are 3 geothermal reservoirs, and the average block density value is 2.25 g/cc. These reservoirs are spread over the Southern area (Cawayan and Tanawon Sector), East area (Boton Sector), and Palayan-Inang Maharang area. Faults or rock intrusions are the limiting factors for the three existing reservoirs. The results obtained from this study will lead to a better understanding of the geothermal system in the study area, in particular, reservoir boundaries, and assist in future geothermal exploration.

**Keywords:** Bac-Man field, Gravity, Modeling, Reservoir, Geothermal

© The Author(s). This is an open access article distributed under the terms of the [Creative Commons Attribution License \(CC BY 4.0\)](https://creativecommons.org/licenses/by/4.0/), which permits unrestricted use, distribution, and reproduction in any medium, provided the original author and source are cited.

[http://dx.doi.org/10.6180/jase.202204\\_25\(2\).0009](http://dx.doi.org/10.6180/jase.202204_25(2).0009)

## 1. Introduction

Geothermal energy is a natural source of heat contained within the Earth, and it can be extracted and used to generate electricity or for heating applications. A geothermal system consists of three elements: a heat source, reservoir rock, and caprock [1]. The Bacon - Manito (Bac-Man) geothermal field is located in the Podcol mountains on Luzon, about 350 km southeast of Manila. The exploration of the Bac-Man geothermal field has been carried out since 1977.

The reservoir model has 23 km<sup>2</sup>, 1500 m depth, and a temperature of 240 °C to 320 °C. Based on geological and geophysical data, a conceptual model of the Bac-Man geothermal system has been made [4]. Tugawin et al. [3]

carried out 2D magneto-telluric (MT) inversion modeling in the Bac-Man field, which shows the existence of 3 (three) geothermal reservoir areas, namely Palayan Bayan, Tikolob, and Malobago areas. These results follow the results of data interpretation of resistivity vertical electric sounding (VES) [5] and Schlumberger Resistivity Traversing (SRT). The reservoir in the Palayan Bayan area has been in production since 1993, while the Tikolob prospect is on the west side of the Bac-Man field, separate from the Palayan Bayan system [3].

The gravity method is applied to determine the geometry of the geothermal reservoir and describe the geological structures that control the system. The gravity method is generally used to describe the subsurface structures that

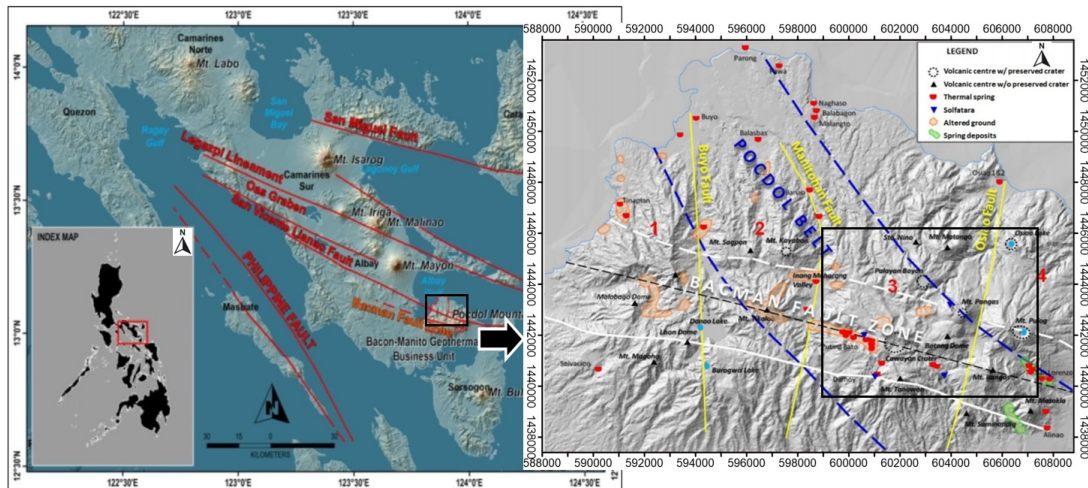


Fig. 1. Map of the study area location and faults structure in the Bac-Man geothermal field [2, 3]

control geothermal systems in geothermal exploration. Certain geothermal reservoirs and their fluid content cause density differences between the geothermal reservoir and the surrounding rock. The basis of the gravity method is the density contrast in the rock. Gravity studies in various regions of the world have yielded valuable results for geothermal exploration, such as the investigation of basement topography in geothermal fields [6]; magma chambers and intrusion bodies associated with heat source from the geothermal system; and faults delineation and fracture zones corresponding to geothermal system reservoirs [7].

Therefore, the gravity method is one of the most economical geophysical methods for modeling geothermal systems. The gravity anomaly interpretation procedure consists of many techniques depending on the quality of the data set and the purpose of the analysis [8]. Gravity anomaly maps are generally analyzed using multiple linear transformations, directional derivative-based techniques, and inverse modeling techniques. Gravity data in the form of a Bouguer anomaly map is used to describe the study area's geological characteristics and subsurface structures.

Observations of gravity at the Earth's surface reflect the superimposed effects of broader and deeper mass variations as well as shallower and more localized changes near the point of observation. This research focuses on the 3D modeling of gravity data to estimate the geothermal reservoir extent and understand the subsurface structure of the geothermal system.

## 2. Bac-Man Geothermal System

The exploration of the Bac-Man geothermal field has been carried out since 1977. Several studies have been carried

out, ranging from geology and geophysics (gravity, magnetic, microearthquake, MT, temperature) to determine the geothermal reservoir, caprocks, heat-source, the geothermal system model, and geothermal potential in the area. The total capacity of the power plant in the Bac-Man area is 150 MWe generated from 4 generating units, namely: Unit I began operating in 1993 and unit II in 1995 which was named Palayang Bayan ( $2 \times 55$  Mwe), in 1996 the Cawayan geothermal plant began operating (20 Mwe), and in 1998 the Unit III power plant in the Botong area began operating (20 Mwe).

The Bac-Man geothermal field is located in the Podcol mountains 350 km southeast of Manila. The local fault system is known as the Bac-Man Fault Zone (BFZ) [9]. The fault zone is indicated by a series of volcanoes that are mostly NW-SE (Fig. 1). Structurally controlled by a fault system, which is believed to be an extension of the San Vicente-Linao Fault (SVLF), is a stretch of the Philippine fault. The most prominent regional geological structure in the area is the San Vicente-Linao Fault in the Northwest-Southeast (NW-SE), which slopes across the Bico Peninsula [10].

The Bac-Man geothermal system is divided into two regions, namely the western and eastern parts of Bac-Man. The eastern part of Bac-Man is further divided into the North Namito lowlands and the Podcol highlands. The Podcol plateau can be divided into eight geographic sectors: Inang Maharang, Putting Bato, Palayan Bayan, Cawayan, Tanawon, Osiao, Bangas, and Botong [10]. Neutral chloride hot springs with a temperature of  $89^{\circ}\text{C}$  -  $96^{\circ}\text{C}$  are found in the lowlands of Manito. In Cawayan and Pangas, Solfatara is found in West Bac-Man, cold to warm, and cold  $\text{SO}_4$  springs are found.

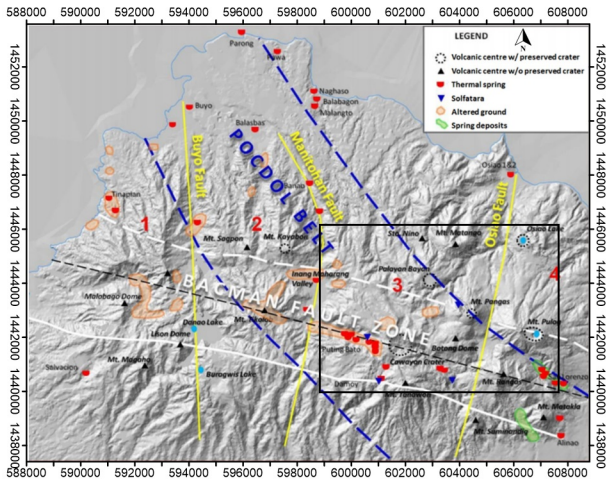


**Fig. 2.** Structure and manifestations at the Bac-Man geothermal field [2]

The most recent volcanic event in the Pocdol highlands occurred more than 40 thousand years ago. That is related to the formation of the Tanawon and Cawayan craters and the Botong and Pangas domes extrusion. The youngest volcanoes generally occur in subsurface areas with high temperatures, permeable formations, and active thermal manifestations (Fig. 2) [10].

Layugan et al. [11] analyzed and interpreted MT data based on 1999 and 2001, which obtained the contour boundaries of the conductive zone's anomaly resistivity as a reservoir area.

An iso-resistivity map at a depth of -1100 m from MSL, which is correlated with the geological structure in the area, shows that the central part of the Bac-Man fault zone has a low resistivity value [3]. The Bac-Man reservoir area covers 26 - 36 km<sup>2</sup>, while the Kayabon reservoir located to the northwest of Bac-Man covers an area of 12 - 18 km<sup>2</sup> (Fig. 3).

The results of this MT study support the results of previous MT research conducted by Layugan et al. [11], which found that the prospect area for the Bac-Man geothermal reservoir is in Botong, Cawayan, and Tikolob. However, the results show a larger area than the results of previous MT studies.

Research related to reservoir temperature was carried out by [4], in which the eastern part of Palayan - Bayan has a high temperature of 326 °C. The temperature contour map at a depth of -1000 meters from MSL is shown in Fig. 4.

### 3. Methods

The gravity data used in this study were 125 points: measurements from 2009 to 2010 [12]. Processing gravity data

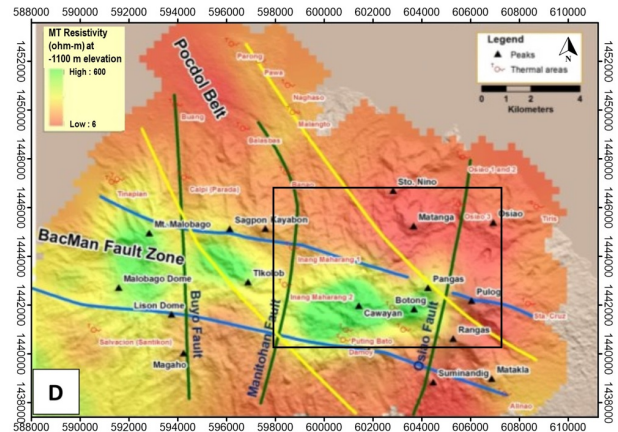


**Fig. 3.** An iso-resistivity map at a depth of -1100 m from MSL which is correlated with the geological structure in the area, shows that the central part of the Bac-Man fault zone has a low resistivity value [3]

includes determination of surface density using the Parasnian and Nettleton method, Bouguer anomaly, Bouguer anomaly filtering, Bouguer anomaly separation, vertical gradient analysis Bouguer anomaly, and Bouguer anomaly modeling.

Analysis and interpretation were carried out to verify the Bac-Man geothermal reservoir area and structures in the area. The analysis and interpretation are carried out by correlating the gravity model with geological data, well data, and other geophysical data. The research flow carried out is shown in Fig. 5.

Density determination was carried out using the Parasnian method and the Nettleton method. The Parasnian method calculations get a value of 2.24 g/cc, while calculations using the Nettleton method for 2 (two) cross-sections get a value of 2.35 g/cc and 2.38 g/cc. When compared with geological conditions in the field, this density value has an appropriate value in research for calculating Bouguer correction and modeling using a density of 2.35 g/cc.

Bouguer anomaly obtained, gravity observation data is performed by gravity theoretic correction at latitude  $\phi$ , free air correction (free air correction), Bouguer correction, and terrain correction. The calculation of the theoretical gravity correction at latitude  $\phi$  uses the International Gravity Formula 1980 equation (Eq. (1)) [13]:

$$g_{\phi} = 978.032,7 \times \left( 1 + 5.302410^{-3} \sin^2 \phi - 5,810^{-6} \sin^2 2\phi \right) \quad (1)$$

Meanwhile, for free air correction, the FAA equation = -0.308 h (mGal/m) is used, which is obtained from the



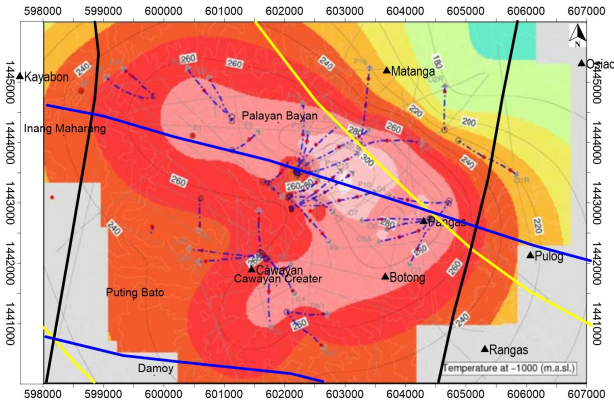


**Fig. 4.** An isoresistivity map at a depth of -1100 m from MSL which is correlated with the geological structure in the area, shows that the central part of the Bac-Man fault zone has a low resistivity value [4]

derivative of the Earth's normal gravity equation in the form of an ellipsoid, namely:

$$g_{\phi,h} = g_{\phi} + \frac{\partial g_{\phi}}{\partial h} h \quad (2)$$

$$\begin{aligned} \frac{\partial g_{\phi}}{\partial h} &= -\frac{2g_{\phi}}{a} (1 + f + m - 2f \sin^2 \phi) \\ &= -0,308 \text{mGal/m} \end{aligned} \quad (3)$$

The Bouguer correction value is calculated using the approaching model for the slab model, namely:

$$Bc = 2\pi G \rho h = 0.04193 \rho h \quad (4)$$

Where  $\rho$  is rock density (g/cc),  $h$  is the height (m), and  $Bc$  is Bouguer correction (mGal).

Terrain corrections were calculated using a combination of the equations given by Nagy (1966) [14] and Kane (1962) [15]. In the calculation of terrain correction, the topographic model is approached with a prism-shaped arrangement of objects measuring 1 km  $\times$  1 km with a height following the area's topography up to a radius of 50 km. The topographical data used is DEM data taken from INA Geoportol [16].

The Bouguer anomaly contains contributions from regional trends resulting from the presence of deep and large structures. The effect of this structure on the gravitational field appears as a large wavelength anomaly, which masks the smaller and shallower effects. To highlight the gravitational anomaly associated with the source of interest for this work, a regional-remaining split of the Bouguer anomaly was performed using the open-source Generic Mapping Tools (GMT) software to map and plot geographic data.

This tool adjusts the trend surface with the grid and calculates the residuals. The regional trend is removed by using the trend-matched grid and removing the polynomial trend in the grid file.

Spectral analysis was carried out to determine the boundary of the regional Bouguer anomaly and the residual area of the study. The results of this spectral analysis are then used to estimate the window width for gravity anomaly filtering. In general, a Fourier transformation is to reconstruct/unravel an arbitrary wave into a sine wave with a variable frequency where the sum of the sine waves is the original waveform [17, 18].

Spectrum analysis is used to determine the depth of the structure of the anomaly. In this study, the analysis of the spectrum analysis used Fourier transform [19], where the results are used to estimate the width of the filtering window.

$$F(g) = 2\pi\gamma m \frac{e^{|k|z_0 - z_1}}{|k|} \quad (5)$$

The energy spectrum of the equation is:

$$E(k) = \frac{4\pi^2 \gamma^2 \rho^2}{|k|^2} e^{-2|k|z} \quad (6)$$

$$\log E(k) = \log (4\pi^2 \gamma^2 \rho^2) - 2|k|z - 2 \log |k| \quad (7)$$

$$\log E(k) = \log A - 2|k|z \quad (8)$$

where  $Z_0$  (depth point),  $Z_1$  (depth mass)  $Z_1 > Z_0$ ,  $k = 2\pi/\lambda$  ((wave number),  $\lambda$  (wavelength),  $g$  (gravity anomaly),  $\rho$  (density).

The separation of regional Bouguer anomalies and residual Bouguer anomalies is a moving average filter with a 5 km  $\times$  5 km window width. The calculation of the moving average is done by averaging the anomaly values for several points of gravity, as shown by the equation:

$$\begin{aligned} \Delta g_{Reg}(i,j) &= \frac{\Delta g(i-n,j-n)}{N} + \frac{\dots + \Delta g(i,j)}{N} \\ &+ \frac{\dots + \Delta g(i+n,j+n)}{N} \end{aligned} \quad (9)$$

where  $n = \frac{N-1}{2}$ , and  $N$  must be an odd number. This average is the regional anomaly, and the residual anomaly is obtained by subtracting the data from the gravity measurement with the regional anomaly [20].

There are several methods for detecting the edges caused by fault structures or geological boundaries. Most of these methods are high-pass filters based on the horizontal and vertical derivatives of the gravity anomaly. One

of these methods is the vertical gradient method, which has been used intensively to delineate contacts of density change from gravity data or pseudo gravity data. Theoretically, this method is derived from Laplace's equation for surface gravity anomalies [19, 21]:

$$\nabla^2 \Delta g = 0 \text{ atau } \frac{\partial^2 \Delta g}{\partial x^2} + \frac{\partial^2 \Delta g}{\partial y^2} + \frac{\partial^2 \Delta g}{\partial z^2} = 0 \quad (10)$$

$$\frac{\partial^2 \Delta g}{\partial z^2} = -\frac{\partial^2 \Delta g}{\partial x^2} - \frac{\partial^2 \Delta g}{\partial y^2} \quad (11)$$

In this study, the Second Vertical Derivative (SVD) anomaly gravity value is calculated using a filtering process, namely through convolution between anomaly gravity and an SVD filter [19].

$$\Delta G_{svd}(\Delta x, \Delta y) = \int_{-\infty}^{\infty} \int_{-\infty}^{\infty} \Delta g(x, y) F(x - \Delta x, y - \Delta y) dx dy \quad (12)$$

where F is the SVD filter according to the above equation and  $\Delta G$  is the gravity anomaly.

Gravity inversion aims to determine the density distribution that would explain the measurements or the shape and dimensions of density variation. However, the inversion of the field gravity data is one of the most ambiguous problems in exploration geophysics studies [22]. Due to data noise and inhomogeneity of geological bodies, inversion of gravity data is usually fraught with difficulties even with reasonably accurate gravity measurements and data reduction.

A 3D inversion modeling of Bouguer Residual anomaly was carried out to obtain a structural model of the Bac-Man Geothermal Field with open source GRAV3D software [23, 24]. The equation used and the calculation of 3D inversion modeling is the subsurface model approach composed of prisms with the amount according to measurement area, data grid, thickness, and depth of objects. The calculation of the gravity response for each prism block uses the Plouff (1976) equation [25]:

$$g = G\Delta\rho \sum_{i=1}^2 \sum_{j=1}^2 \sum_{k=1}^2 \mu_{ijk} \left[ z_k \arctan \frac{x_i y_i}{z_k R_{ijk}} - x_i \log(R_{ijk} + y_i) - y_i \log(R_{ijk} + x_i) \right] \quad (13)$$

where:  $R_{ijk} = \sqrt{x_i^2 + y_j^2 + z_k^2}$ ;  $\mu_{ijk} = (-1)^i (-1)^j (-1)^k$

#### 4. Result and Discussions

The Bouguer anomaly in the Bac-Man geothermal field has a value of 18 - 41 mGal, with a high anomaly in the west to

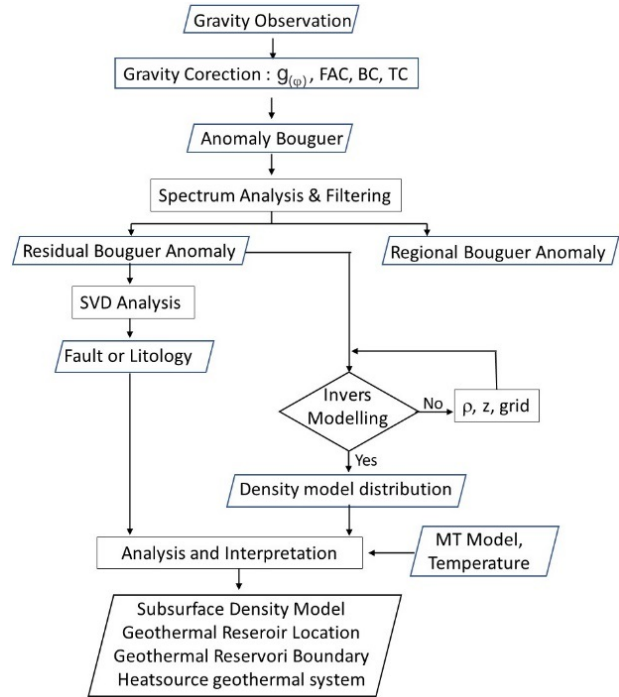


Fig. 5. Flowchart of research in determining the boundary of a geothermal reservoir

the northwest and a little in the middle, while the anomaly is low in the middle. The high anomaly in the Northwest part is probably related to the geothermal system's heat source in the Bac-Man field. The low anomaly in the middle part flanking the high anomaly is probably related to a reservoir in the area (Fig. 6)

The spectrum analysis was carried out by cross-sectioning the Bouguer anomaly as many as 5 trajectories with a point interval of 250 m (Fig. 7). The spectrum analysis result from 5 lines of Bouguer anomaly shows that the average regional Bouguer anomaly depth is 2500 meters (Fig. 8). Based on these results, the separation of regional Bouguer anomalies and residual Bouguer anomalies is a moving average filter with a 5 km x 5 km window width.

The residual Bouguer anomaly map from the Bouguer anomaly filtering using the moving average method with windows 5 km x 5 km is shown in Fig. 9. Residual Bouguer anomaly maps have values from -12 mGal to 9 mGal. High anomalies occupy the eastern and central parts of the study area, surrounded by low anomalies in the north, south, and east. This area that occupies a low anomaly is probably the geothermal reservoir area of the Bac-Man field.

This is following the MT geophysical data and well data. There are 3 low anomaly closures in the middle, which are separated by high anomalies. It can be interpreted that the geothermal reservoir in the Bac-Man field may be

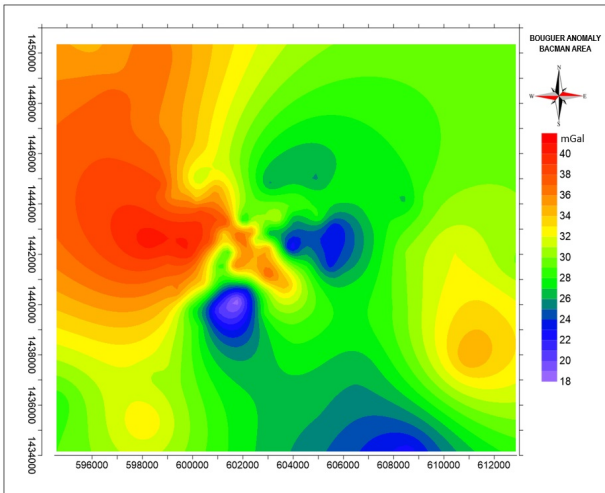


**Fig. 6.** Map of the Bouguer anomaly of the Bac-Man geothermal field area

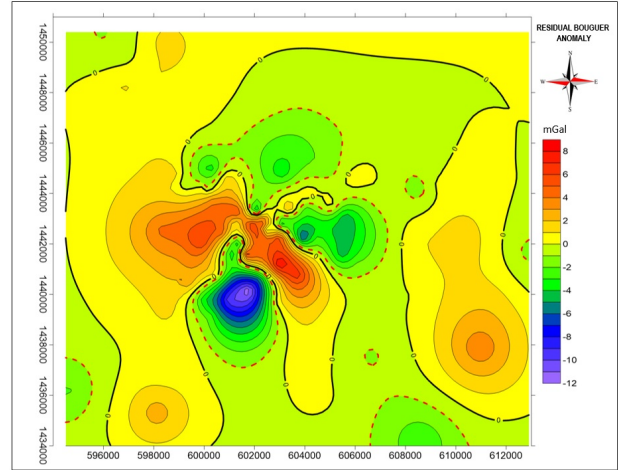


**Fig. 9.** Map of the Bouguer Residual anomaly of the Bac-Man geothermal field

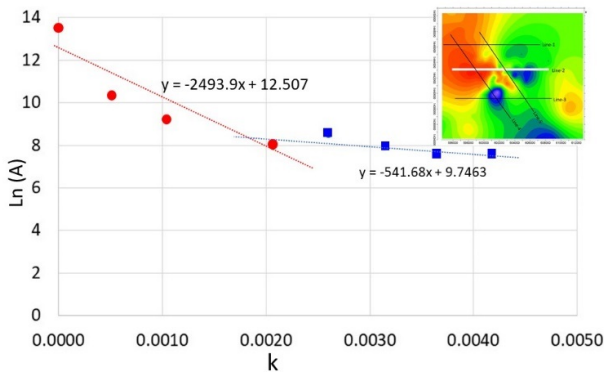


**Fig. 7.** Bouguer anomaly spectrum analysis to determine the depth limits of regional and residual anomalies. The spectrum analysis results for line 2 get the depth limit value of the residual regional Bouguer anomaly of  $2483.9 = 2500$  m.

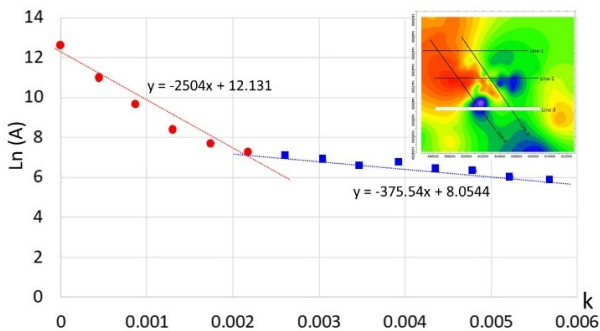


**Fig. 8.** Bouguer anomaly spectrum analysis to determine the depth limits of regional and residual anomalies. The spectrum analysis results for line 2 get the depth limit value of the residual regional Bouguer anomaly of  $2504 = 2500$  m.

divided into 3 reservoirs, namely the north, south, and east. Reservoirs may be separated from one another by fault structures or the presence of intrusion in the area.

This study's SVD filter is the Elkins (1951) [21] type. The SVD map compiled Bouguer Residual anomaly with low residual Bouguer anomaly contours. The boundaries of the Bac-Man field geothermal prospects from the MT data are shown in Fig. 10.

Data compilation of low Bouguer Residual anomaly, Bouguer Residual anomaly SVD, and reservoir prospect boundaries derived from MT data were carried out to identify a reservoir in the area. In general, geothermal reservoirs will have a low Bouguer anomaly because a good geothermal reservoir will have a high porosity value and high permeability. The reservoir rock will have a low density. The SVD map of Bouguer Residual anomaly compiled with: Low Residual Bouguer anomaly, reservoir area boundary derived from MT data, and reservoir prospect area derived from Bouguer Residual anomaly data is shown in Fig. 10.

The figure shows that the reservoir locations of the four data provide the same results. The reservoir areas identified from the Bouguer Residual anomaly data and the Bouguer Residual SVD anomaly provide more detailed results, namely the Bac-Man geothermal reservoir is separated into 3 areas, namely: the Cawayan and Tanawon sectors in the south, the Boton sector, which is located in the east, and the East sector Palayang. This result is also supported by the high temperature in the area, where the highest temperature is in the Palayang sector.

The temperature distribution map at 1200 m from MSL shows that the center has a high temperature, probably due to intrusion. This intrusion follows the high residual



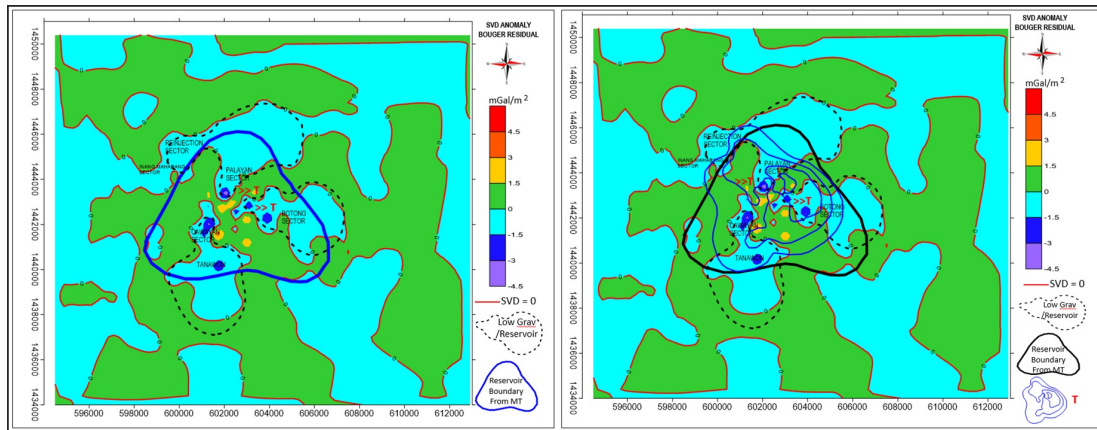


**Fig. 10.** SVD map of the residual Bouguer anomaly overlaid with the reservoir area derived from MT data and the reservoir prospect area derived from the Bouguer Residual anomaly data.

gravity anomaly pattern in the area, where the intrusion is also a barrier from 3 reservoir locations in the area. Based on drilling data in the Bac-Man geothermal area, dike and intrusive rocks such as monzogabbro, monzodiorite, and epidote have high-density characteristics (gabbro = 3.03 g/cc; amphibolite = 2.96 g/cc) [26]. These dike and intrusion zones have high temperatures interpreted as heat sources of the Bac-Man geothermal system [27]. The high gravity anomaly is associated with the presence of high density below the surface.

The results of Bouguer Residual anomaly 3D inversion modeling using the Grav3D program are shown in Fig. 11. The 3D inversion modeling result, density distribution model, shows high and low density in the middle of the study area with a value of 2 g/cc to 2.9 g/cc. The model is then carried out by slicing the selected paths, which will be compared and correlated with temperature data models, MT cross-sectional models, structural models, and others to obtain a structural model.

The density distribution model resulting from the 3D Bouguer anomaly residual inversion which is correlated with the cross-sectional temperature model and the intrusion structure on the NW-SE trajectory is shown in Fig. 12. The 3D Bouguer anomaly residual inversion result correlated with the temperature section model [27], and the intrusion structure shows a good correlation. The presence of intrusion is correlated with high density in the area. Likewise, the SVD section indicates that the intrusion is no single but separated into three parts according to the model derived from well data and temperature data.

The density distribution model resulting from the 3D Bouguer anomaly residual inversion which is correlated with the temperature cross-section model and the intrusion structure on the NE-SW trajectory is shown in Fig.

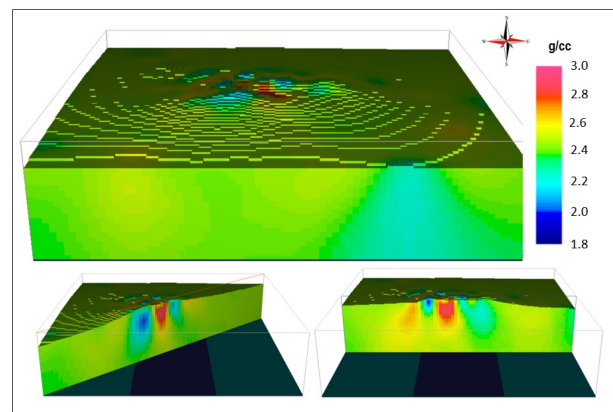


**Fig. 11.** The subsurface density distribution model from the 3D inversion modeling result of Bouguer residual anomaly in Bac-Man geothermal field

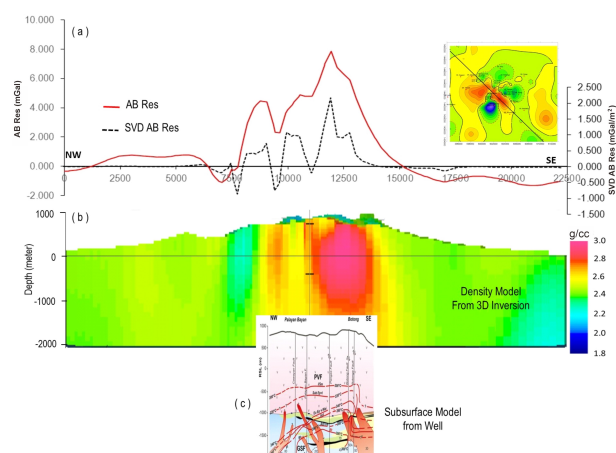


**Fig. 12.** The cross-section of the density distribution model resulting from the 3D Bouguer residual anomaly inversion correlated with the temperature and intrusion structure cross-sectional model for the NW-SE trajectory [27].

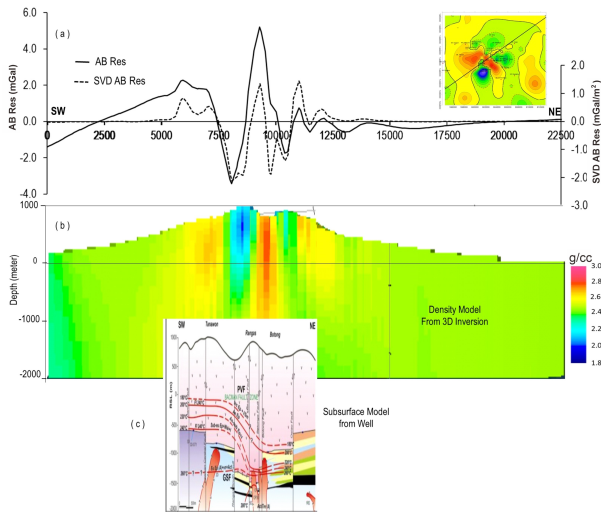


**Fig. 13.** The cross-section of the density distribution model resulted from the Bouguer Residual anomaly 3D inversion which is correlated with the temperature and intrusion structure cross-sectional model for the NE-SW trajectory [27].

13 . The 3D Bouguer anomaly residual inversion result, which correlated the temperature cross-section model and the intrusion structure, shows a good correlation. The presence of intrusion correlates with high density in the area. Likewise, the SVD section indicates that the intrusion is no single but separated into two parts according to the model derived from well data and temperature data.

The model is correlated with: the boundary of the geothermal reservoir area delineated from the MT results, the division of the geothermal sector, and volcanoes that control the geothermal system in the Bac-Man field. The results of the correlation analysis between the cut density distribution models for density 2.1 g/cc - 2.4 g/cc (interpreted as a geothermal reservoir) and the reservoir prospect boundary derived from MT indicate that the reservoir locations have similarities. However, the reservoir area derived from the gravity model is broader and in more detail.

The gravity modeling shows that the geothermal reservoir in the Bac-Man field is divided into 3 areas: the southern part (Cawayan and Tanawon sector), the eastern part (Boton sector), and the northern part (Palayan-Inang Maharang sector). Each reservoir area is separated by the presence of fault structures or intrusions in the area. The division of the 3 reservoir areas follows the well data and the results of reservoir modeling research in the area. That the geothermal reservoir area of the Bac-Man field is divided into 3 sectors, namely the south (Cawayan and Tanawon sectors), the east (Boton sector), and the north (the North

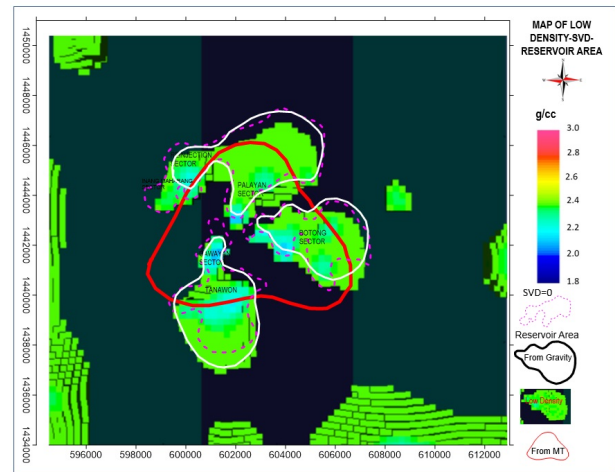


**Fig. 14.** The density distribution model of Bouguer Residual anomaly 3D inversion modeling shows densities 2.1 g/cc - 2.4 g/cc. The model is correlated with: geothermal reservoir area boundaries delineated from the MT results, SVD = 0 maps, the division of geothermal areas, and volcanoes that control the geothermal system in the Bac-Man field.

sector). Palayan-Inang Maharang) (Fig. 14 ). The reservoir sectors are separated by intrusion in the study area and supported by the reservoir temperature in the area with a higher temperature than the surrounding area.

## 5. Conclusions

Based on the results of gravity research on the Bac-Man geothermal field supported by geological data, well data, MT data, and temperature data, several conclusions can be drawn regarding the Bac-Man geothermal field, namely:

1. Bouguer anomaly in the study area has a value of 18 - 41 mGal, with a high anomaly in the west to the north-west and a little in the middle, while the anomaly is low in the middle. From the Bouguer anomaly spectrum analysis, it is found that the Bouguer Regional and Residual anomaly limits are at a depth of 2500 m.
2. Residual Bouguer anomaly calculated using a moving average filter with windows 5 km × 5 km shows that the residual Bouguer anomaly has a value of -12 mGal to 9 mGal with high anomalies occupying the eastern and central parts. There are 3 low anomaly closures in the middle that are separated by high anomalies. The geothermal reservoir in the Bac-Man field may be divided into 3 reservoirs: the North, South, and East.
3. The density distribution model from the 3D inversion modeling shows that the density distribution model



cut for density 2.1 g/cc - 2.4 g/cc correlates with the MT reservoir boundary. However, the reservoir area derived from the gravity model is broader and more detailed. The results of gravity modeling show that the geothermal reservoir in the Bac-Man field is divided into 3 areas: the southern part (Cawayan and Tanawon sector), the eastern part (Boton sector), and the northern part (Palayan - Inang Maharang sector) where each reservoir area is separated by the presence of fault structures or intrusions in the area.

The division of the 3 reservoir areas follows the well data and the results of reservoir modeling research in the area. The reservoir sectors are separated by intrusion in the area. Temperature data also support this, showing that the area has a higher temperature than the surrounding area.

4. Detailed reservoir boundaries, especially the outer reservoir boundaries, suggest adding more detailed gravity measurement points in the north, east, and south.

### Acknowledgments

We want to thank all those who have helped implement this research, especially the Geophysical Engineering Department, Faculty of Engineering, University of Lampung.

### References

- [1] S. Zarrouk and K. Mclean. *Geothermal Well Test Analysis*. 2019. DOI: [10.1016/c2017-0-02723-4](https://doi.org/10.1016/c2017-0-02723-4).
- [2] J. R. Africa. *1D Inversion of MT and TEM Data With Application of Soundings From Krýsuvík, Sw-Iceland and a Review of MT/TEM Data From Bac-Man Geothermal Project, Central Philippines*. Tech. rep. 5. Reykjavik, 2013, 33.
- [3] R. J. Tugawin, D. M. Rigor, C. E. F. Los Baños, and D. B. Layugan, (2015) "Resistivity Model Based on 2D Inversion of Magnetotelluric Sounding Data in Bacon-Manito, Southern Luzon, Philippines" **Proceedings World Geothermal Congress 2015** (April): 1–6.
- [4] J. J. C. Austria. *Production Capacity Assessment of the Bacon-Manito Geothermal Reservoir, Philippines*. Tech. rep. 2. Department of Mechanical and Industrial Engineering, University of Iceland, 2008, 89.
- [5] T. A. Abiye and Tigistu Haile, (2008) "Geophysical exploration of the Boku geothermal area, Central Ethiopian Rift" **Geothermics** 37(6): 586–596. DOI: [10.1016/j.geothermics.2008.06.004](https://doi.org/10.1016/j.geothermics.2008.06.004).
- [6] S. Soengkono. "Deep interpretation of gravity and airborne magnetic data of the Central Taupo volcanic zone". In: *New Zealand Geothermal Workshop Proceedings (21-23 November 2011)*. 1955. 2011.
- [7] P. Represas, F. A. Monteiro Santos, J. Ribeiro, J. A. Ribeiro, E. P. Almeida, R. Gonçalves, M. Moreira, and L. A. Mendes-Victor, (2013) "Interpretation of gravity data to delineate structural features connected to low-temperature geothermal resources at Northeastern Portugal" **Journal of Applied Geophysics** 92: 30–38. DOI: [10.1016/j.jappgeo.2013.02.011](https://doi.org/10.1016/j.jappgeo.2013.02.011).
- [8] W. J. Hinze, R. R. B. von Frese, and A. Saad. *Gravity and magnetic exploration: principles, practices and exploration*. Cambridge University Press, 2013, 512.
- [9] J. J. T. Dimabayao, M. C. Rowe, and S. Barker, (2019) "Stable isotope systematics of fluids and epidote in the Bacon-Manito Geothermal Field, Philippines: Indicators of fluid origin and evolution" **Geothermics** 80: 31–43. DOI: [10.1016/j.geothermics.2019.02.009](https://doi.org/10.1016/j.geothermics.2019.02.009).
- [10] A. Reyes, M. Delfin, and E. Bueza. "PETROLOGICAL IDENTIFICATION OF MULTIPLE HEAT SOURCES IN THE BACON-MANITO GEOTHERMAL SYSTEM, TIII PHILIPPINES". In: *Proceedings World Geothermal Congress*. Florence, 1995, 713–717.
- [11] D. B. Layugan, D. M. Rigor, N. A. Apuada, R. E. R. Olivar, M. City, and S. Leyte. "Magnetotelluric ( MT ) Resistivity Surveys in Various Geothermal Systems in Central Philippines". In: *Proceedings World Geothermal Congress*. 2000. April. Antalya, 2005, 24–29.
- [12] J. L. Monasterial. *Microgravity Survey in 2009-2010 Around Bacman Geothermal Field, Philippines - Gravity Corrections and Interpretations*. Tech. rep. 23. Reykjavik, 2015, 22.
- [13] B. H. Wellenhof and H. Moritz. *Physical Geodesy*. Austria: SpringerWienNewYork, 2005, 412. arXiv: [arXiv: 1011.1669v3](https://arxiv.org/abs/1011.1669v3).
- [14] D. Nagy, (1966) "The prism method for terrain corrections using digital computers" **Pure and Applied Geophysics PAGEOPH** 63(1): 31–39. DOI: [10.1007/BF00875156](https://doi.org/10.1007/BF00875156).
- [15] M. Kane, (1962) "A Comprehensive System of Terrain Corrections Using A Digital Computer" **GEOPHYSICS** XXVII(4): 455–462.
- [16] Ina-Geoportal. *DEM Data*.
- [17] B. K. Bhattacharyya and L. K. Leu, (1977) "Spectral Analysis of Gravity and Magnetic Anomalies Due To Rectangular Prismatic Bodies." **Geophysics** 42(1): 41–50. DOI: [10.1190/1.1440712](https://doi.org/10.1190/1.1440712).

- [18] G. K. Ghosh and C. L. Singh, (2014) “Spectral analysis and Euler deconvolution technique of gravity data to decipher the basement depth in the Dehradun-Badrinath area” **Journal of the Geological Society of India** 83(5): 501–512. DOI: [10.1007/s12594-014-0077-3](https://doi.org/10.1007/s12594-014-0077-3).
- [19] R. J. Blakely. *Potential Theory in Gravity and Magnetic Applications*. Cambridge University Press, 1995, 441. DOI: [10.1017/CBO9780511549816](https://doi.org/10.1017/CBO9780511549816).
- [20] I. Setiadi, B. Styanta, and B. Widijono, (2010) “Delineasi cekungan sedimen sumatra selatan berdasarkan analisis data gaya berat” **Jurnal Geologi dan Sumber Daya Mineral** 20(April): 93–106.
- [21] T. A. Elkins, (1951) “The second derivative method of gravity interpretation” **Geophysics** 16(1): 29–50. DOI: [10.1190/1.1437648](https://doi.org/10.1190/1.1437648).
- [22] Z. Zhu, X. Lei, N. Xu, D. Shao, X. Jiang, and X. Wu, (2020) “Integration of 3D geological modeling and geothermal field analysis for the evaluation of geothermal reserves in the Northwest of Beijing Plain, China” **Water (Switzerland)** 12(3): DOI: [10.3390/w12030638](https://doi.org/10.3390/w12030638).
- [23] E. Januari, D. Santoso, and A. F. M. Ulum. “Gravity Survey in Pandan Mountain - East Java , Indonesia Gravity Survey in Pandan Mountain – East Java , Indonesia”. In: *IOP Conf. Series: Journal of Physics: Conf. Series*. 2019, 11. DOI: [10.1088/1742-6596/1204/1/012006](https://doi.org/10.1088/1742-6596/1204/1/012006).
- [24] A. Adhi, W. Suryanto, and M. Sarkowi, (2018) “GRAV3D Validation using Generalized Cross- Validation ( GCV ) Algorithm by Lower Bounds Approach for 3D Gravity Data Inversion” **Scientific Journal of Informatics** 5(2): 271–277.
- [25] D. Plouff, (1976) “Gravity and Magnetic Fields of Polygonal Prisms and Application to Magnetic Terrain Corrections” **GEOPHYSICS** 41(4): 727–741.
- [26] W. Telford, L. P. Geldart, and R. Sheriff. *Applied Geophysics: Second Edition*. Cambridge University Press, 1990, 760.
- [27] S. Ramos and B. Santos. “Updated Hydrogeological Model of the Bacon-Manito Geothermal Field , Philippines”. In: *Proceedings of 37th Stanford Geothermal Workshop*. California, 2012, 1–4.